PHYSICAL REVIEW D **73,** 044002 (2006)

Quasinormal modes of brane-localized standard model fields

P. Kanti*

Department of Mathematical Sciences, University of Durham, Science Site, South Road, Durham DH1 3LE, United Kingdom

R. A. Konoplya†

Instituto de Física, Universidade de São Paulo, C.P. 66318, 05315-970, São Paulo-SP, Brazil

(Received 21 December 2005; published 3 February 2006)

We present here a detailed study of the quasinormal spectrum of brane-localized standard model fields in the vicinity of D-dimensional black holes. A variety of such backgrounds [Schwarzschild, Reissner-Nordström and Schwarzschild-(anti−)de Sitter] are investigated. The dependence of the quasinormal spectra on the dimensionality D, spin of the field s, and multipole number ℓ is analyzed. Analytical formulas are obtained for a number of limiting cases: in the limit of large multipole number for Schwarzschild, Schwarzschild-de Sitter, and Reissner-Nordström black holes, in the extremal limit of the Schwarzschild-de Sitter black hole, and in the limit of small horizon radius in the case of Schwarzschild-anti−de Sitter black holes. We show that an increase in the number of hidden, extra dimensions results in the faster damping of all fields living on the brane, and that the localization of fields on a brane affects the quasinormal spectrum in a number of additional ways, both direct and indirect.

DOI: 10.1103/PhysRevD.73.044002 PACS numbers: 04.30.Nk, 04.50.+h

I. INTRODUCTION

Upon an external perturbation of a black hole background, realized either through the addition of a field or by perturbing the metric itself, the gravitational system enters a phase of damping oscillations, or quasinormal ringing [1,2] as it is alternatively called. During this phase, the frequency of the field consists of a real part ω_{Re}, that drives the field oscillations, and of an imaginary part ω_{Im}, that causes the simultaneous damping of these oscillations. The smaller ω_{Im} is, the longer the damping time, and therefore certain quasinormal modes (QNMs) can dominate the spectrum at very late times after the initial perturbation, thus governing the dynamical evolution of the black hole.

The spectrum of quasinormal modes has been the subject of an intensive study over the years, not only for their theoretical interest, but also due to the fact that their potential experimental detection could lead to the discovery of black holes. In a four-dimensional context, they have been both numerically and analytically studied for a variety of black hole backgrounds [3]. Among the different species of fields, the quasinormal modes associated to gravitons, generated by metric perturbations, were particularly looked at, for the simple reason that gravitational QNMs originating from astrophysical black holes could potentially be observed with the help of gravitational wave detectors [1,2]. Unfortunately, such an experimental confirmation has not been obtained up to now.

A few years ago, the landscape in gravitational physics changed with the formulation of theories postulating the existence of additional spacelike dimensions in nature [4,5]. According to these theories, all standard model (SM) particles (scalars, fermions, and gauge bosons) are restricted to live on a $(3 + 1)$-dimensional hypersurface—a brane—embedded in the higher-dimensional "bulk." Gravitons can propagate both on and off the brane, with the same being true for other particles, like scalars, that carry no charges under the standard model gauge group. This geometrical setup protects the accurately observed properties of SM fields from being altered due to the presence of extra dimensions while opening the way for the study of new gravitational backgrounds.

The theory with large extra dimensions [4] predicts the existence of d additional spacelike compact dimensions, all having—in the simplest case—the same size L. Black holes produced by the gravitational collapse of matter on the brane would naturally extend off the brane, being gravitational objects. Whereas macroscopic astrophysical black holes extend mainly along the usual three, noncompact spatial dimensions, thus being effectively four-dimensional objects, microscopic black holes with a horizon radius $r_H \ll L$ would virtually live in a noncompact spacetime with $D = 4 + d$ dimensions in total. Higher-dimensional generalizations of four-dimensional black hole solutions [6,7], derived previously, came back in the spotlight, and the study of the QNMs associated with these higher-dimensional backgrounds soon became the subject of a renewed research activity [8].

One of the most exciting predictions of the theory with large extra dimensions [4] is that such microscopic black holes may be created on ground-based accelerators during the collision of highly energetic particles with center-of-mass energy $\sqrt{s} > M_*$ [9]. The energy scale M_* denotes the fundamental Planck scale of the higher-dimensional

*Electronic address: panagiota.kanti@durham.ac.uk
†Electronic address: konoplya@fma.if.usp.br

gravitational theory that becomes effective at distances $r < L$. This scale can be much lower than the four-dimensional Planck scale $M_{\rm Pl}$, even as low as 1 TeV; therefore, trans-Planckian collisions can be realized easily at next-generation particle colliders. What is of the utmost importance is the fact that these tiny black holes, contrary to what happens in the case of macroscopic black holes, will be created in our neighborhood in a controlled experiment inside a laboratory; therefore, their detection, either through the emission of Hawking radiation or the detection of their QNMs spectrum, will be substantially more favored. In the latter case, the spectrum of QN modes associated with SM fields living in our brane will be the most important of all due to the well-developed techniques for the detection of fermions and gauge bosons, compared to the ones for the up-to-now elusive gravitons.

In this work, we attempt to fill the gap in the existing literature by presenting a comprehensive study of the QN modes associated with the brane-localized SM fields. We will examine a variety of higher-dimensional black hole backgrounds, namely, the Schwarzschild, Reissner-Nordström, and Schwarzschild-(anti–)de Sitter, all described by the same static, spherically-symmetric line element with a single metric function. The spectrum of the QN modes for scalars, fermions, and gauge bosons will be derived in each case, as a function of the dimensionality of spacetime, the multipole number and additional fundamental parameters such as the bulk cosmological constant and charge of the black hole. In what follows, we will be assuming that the black hole is characterized by a mass $M_{\rm BH}$ that is at least a few orders of magnitude larger than the fundamental scale of gravity M_*, so that quantum corrections can be safely ignored. Also, in order to avoid a hierarchy problem, the brane self-energy can be assumed naturally to be of the order of the fundamental Planck scale M_* and thus much smaller than $M_{\rm BH}$; therefore, its effect on the gravitational background also can be ignored.

In Sec. II, we present the theoretical framework for our analysis and the equations of motion for the SM fields propagating in the brane background. Section III focuses on the associated QNM spectrum in the case of an induced-on-the-brane D-dimensional Schwarzschild black hole and investigates the dependence of the spectrum on the dimensionality of spacetime, spin of the particle, and multipole number. In Sec. IV we proceed to consider the QN modes of SM particles propagating on a brane embedded in a charged D-dimensional Reissner-Nordström black hole, and the effect of the black hole charge on the QN spectrum is examined in detail. The spectra of QNMs for brane-localized SM fields in the background of a D-dimensional Schwarzschild-de Sitter and Schwarzschild-anti–de Sitter black hole are derived in Secs. V and VI, respectively, and the role of the bulk cosmological constant is investigated. We present our conclusions in Sec. VII.

II. MASTER EQUATION FOR PROPAGATION OF FIELDS ON THE BRANE

As mentioned above, in this work we will concentrate on spherically-symmetric higher-dimensional black hole backgrounds arising under the assumption of the existence of $d = D - 4$ additional, compact spacelike dimensions in nature. A large variety of such backgrounds may be described by a unique line element of the form

$$ds^2 = -h(r)dt^2 + \frac{dr^2}{h(r)} + r^2 d\Omega_{d+2}^2, \tag{1}$$

where $d\Omega_{d+2}^2$ is the area of the $(d+2)$-dimensional unit sphere given by

$$d\Omega_{d+2}^2 = d\theta_{d+1}^2 + \sin^2\theta_{d+1}(d\theta_d^2 + \sin^2\theta_d \times (\ldots + \sin^2\theta_2(d\theta_1^2 + \sin^2\theta_1 d\varphi^2)\ldots)), \tag{2}$$

with $0 < \varphi < 2\pi$ and $0 < \theta_i < \pi$, for $i = 1, \ldots, d+1$. The radial-dependent metric function $h(r)$ may now be assumed to take the form

$$h(r) = 1 - \frac{\mu}{r^{D-3}}, \tag{3}$$

describing a higher-dimensional, neutral black hole formed in a flat, empty space [6], with the parameter μ related to the ADM mass of the black hole through the relation

$$\mu = \frac{\kappa_D^2 M_{\rm BH}}{(D-2)\pi^{(D-1)/2}}\Gamma\left[\frac{D-1}{2}\right]. \tag{4}$$

Alternatively, it may be taken to be

$$h(r) = 1 - \frac{\mu}{r^{D-3}} + \frac{Q^2}{r^{2(D-3)}}, \tag{5}$$

in the case of a higher-dimensional, charged black hole [7] with Q^2 the electromagnetic charge. Finally, it may be written as

$$h(r) = 1 - \frac{\mu}{r^{D-3}} - \frac{2\kappa_D^2\Lambda r^2}{(D-1)(D-2)} \tag{6}$$

to describe a Schwarzschild-(anti–)de Sitter black hole formed in a $(d+4)$-dimensional spacetime with the presence of a (negative) positive cosmological constant Λ [6]. In the above expressions, $\kappa_D^2 = 8\pi G = 8\pi/M_*^{D-2}$ stands for the higher-dimensional Newton's constant.

In what follows, we will study all three types of black hole backgrounds and derive exact numerical results for the associated quasinormal modes of all species of standard model fields: scalars, fermions, and gauge bosons. According to the assumptions of the model [4], all SM fields are localized to a brane embedded in the bulk (1). Since a potential observer also lives on the brane, the study of the QNMs of brane-localized fields is the most phenomenologically interesting one. To this end, we need first to determine the line element of the background in which the brane-localized modes propagate. This can be found by

fixing the values of the additional angular coordinates, describing the compact d dimensions, to $\theta_i = \pi/2$ [10,11]. This results in the projection of the higher-dimensional background (1) onto the brane, and in the induced-on-the-brane line element

$$ds^2 = -h(r)dt^2 + \frac{dr^2}{h(r)} + r^2(d\theta^2 + \sin^2\theta d\varphi^2). \quad (7)$$

As the projection clearly affects only the angular part of the higher-dimensional line element given in Eq. (2), the metric function $h(r)$ remains unaffected and is still given by Eq. (3), (5), or (6). Note that, although the additional, spacelike dimensions have been projected out, the induced-on-the-brane line element carries an explicit dependence on the number and content of extra dimensions through the metric function $h(r)$.

The next step in our analysis is the derivation of the equations of motion of the various species of fields propagating on the brane. This task was performed in [12] (see also [13]) for fields with spin $s = 0, 1/2$, and 1, by using the Newman-Penrose method [14,15]. For a field with spin s, the following standard factorization was employed

$$\Psi_s(t, r, \theta, \varphi) = e^{-i\omega t}e^{im\varphi}\Delta^{-s}P_s(r)S_s(\theta), \quad (8)$$

where $\Delta = hr^2$, and $S_s(\theta)$ are the spin-weighted spherical harmonics [16]. As it was shown in [12], the radial and angular parts of each equation are decoupled and take the ''master'' form

$$\Delta^s \frac{d}{dr}\left(\Delta^{1-s}\frac{dP_s}{dr}\right) + \left(\frac{\omega^2 r^2}{h} + 2is\omega r - \frac{is\omega r^2 h'}{h} - \tilde{\lambda}\right)P_s = 0, \quad (9)$$

and

$$\frac{1}{\sin\theta}\frac{d}{d\theta}\left(\sin\theta\frac{dS_s}{d\theta}\right) + \left[-\frac{2ms\cot\theta}{\sin\theta} - \frac{m^2}{\sin^2\theta} + s - s^2\cot^2\theta + \lambda\right]S_s = 0, \quad (10)$$

respectively. Following [17], these Teukolsky-like equations hold for the upper component $s = |s|$ of all fields with spin $s = 0, 1/2$, and 1. The constant $\tilde{\lambda}$ appearing in the radial equation is related to the angular eigenvalue λ as follows:

$$\tilde{\lambda} \equiv \lambda + 2s = \ell(\ell + 1) - s(s - 1). \quad (11)$$

By choosing the desired expression for the metric function $h(r)$ from the set of Eqs. (3), (5), and (6), Eqs. (9) and (10), then, describe the motion of a particle with spin s localized on a brane embedded in a higher-dimensional Schwarzschild, Reissner-Nordström, and Schwarzschild-(anti–)de Sitter background, respectively.

A. Alternative form: one-dimensional wave equation

For the purpose of calculating the QNMs of brane-localized fields living in a general, spherically-symmetric background of the form (7), studying the radial Eq. (9) will be adequate. In what follows, we will rewrite this equation in a more convenient form, namely, in the form of a one-dimensional Schrödinger (or wavelike) equation, and derive the form of the corresponding effective potential. To this end, we follow the analysis performed in [18] and define a new radial function and a new (''tortoise'') coordinate according to

$$P_s = r^{2(s-1/2)}Y_s, \qquad \frac{dr_*}{dr} = \frac{1}{h}. \quad (12)$$

Then, Eq. (9) takes the form

$$\left(\frac{d^2}{dr_*^2} + \omega^2\right)Y_s + \mathcal{P}\left(\frac{d}{dr_*} + i\omega\right)Y_s - \mathcal{Q}Y_s = 0, \quad (13)$$

where we have defined

$$\mathcal{P} = s\left(\frac{4h}{r} - \frac{\Delta'}{r^2}\right), \quad (14)$$

and

$$\mathcal{Q} = \frac{h}{r^2}\left\{\tilde{\lambda} - (2s - 1)(s - 1)\left(2h - \frac{\Delta'}{r}\right)\right\}. \quad (15)$$

By defining further

$$Y_s = hZ_s + 2i\omega\left(\frac{d}{dr_*} - i\omega\right)Z_s, \quad (16)$$

Eq. (13) can now be written as a one-dimensional Schrödinger equation

$$\left(\frac{d^2}{dr_*^2} + \omega^2\right)Z_s = V_sZ_s. \quad (17)$$

The effective potential V_s is found to be spin dependent and given by the expression

$$V_{s=1} = \frac{h}{r^2}\ell(\ell + 1), \quad (18)$$

for spin-1 particles, where we have used Eq. (11), and

$$V_{s=1/2} = hk\left[\frac{k}{r^2} \mp \frac{d}{dr}\left(\frac{\sqrt{h}}{r}\right)\right], \quad (19)$$

for spin-$1/2$ particles, where

$$k = \sqrt{\ell(\ell + 1) + 1/4} = 1, 2, 3, \ldots \quad (20)$$

For spin-0 particles, the quantity $\mathcal{P}$ defined in Eq. (14) vanishes trivially, and the equation for Y_s (13) automatically takes a wavelike form, with potential

$$V_{s=0} = h\left[\frac{\ell(\ell + 1)}{r^2} + \frac{h'}{r}\right]. \quad (21)$$

The above results hold for any D-dimensional, spherically-

symmetric black hole (Schwarzschild, Reissner-Nordström, and Schwarzschild-dS/AdS) projected onto the brane, upon choosing the correct value of the metric function $h(r)$.

III. NEUTRAL NONROTATING BLACK HOLE: WKB VALUES OF BRANE QNMS

For a D-dimensional Schwarzschild black hole background, the effective potentials V_s, seen by scalars, fermions, and gauge bosons propagating on the embedded brane, have the form of a positive-definite potential barrier that attains its maximum value close to the black hole while it vanishes at the event horizon ($r_* = -\infty$) and spatial infinity ($r_* = +\infty$). According to Eq. (17) then, the solution for all types of fields in these two asymptotic regimes can be written in terms of incoming and outgoing plane waves. If we write the quasinormal frequency as $\omega = \omega_{\mathrm{Re}} - i\omega_{\mathrm{Im}}$, under the choice of the positive sign for ω_{Re}, the QNMs for all standard model particles propagating on the brane satisfy the boundary conditions [1,2]

$$\Psi_s(r_*) \approx C_{\pm} \exp(\pm i\omega r_*) \quad \text{as} \quad r_* \to \pm\infty, \tag{22}$$

corresponding to purely ingoing waves at the event horizon and purely outgoing waves at spatial infinity.

The fact that the effective potentials V_s have the form of a positive-definite potential barrier also allows us to use the well-known WKB method in order to find the various QNMs with a significantly good accuracy. The WKB formula for QN frequencies has the form:

$$i\frac{\omega^2 - V_0}{\sqrt{-2V_0''}} - L_2 - L_3 - L_4 - L_5 - L_6 = n + \frac{1}{2}, \tag{23}$$

where V_0 is the height of the potential at its maximum point, located at r_0, and V_0'' its second derivative with respect to the tortoise coordinate at the same point. The lower terms L_2 and L_3 can be found in [19], while the higher ones L_4, L_5, and L_6 in [20]. Finally, the symbol n in the above formula denotes the various overtones.

By using the above formula, we have calculated the QNMs for all species of SM fields for various values of the dimensionality D of the spacetime, multipole moment ℓ, and overtone number n. In Tables I, II, and III we display, as illustrative examples, the QNMs for scalars, fermions, and gauge bosons, respectively, for $D = 5$ and $D = 6$, and for $n \leq \ell$ up to $\ell = 3$. The only numerical results available in the literature for QN modes of brane-localized fields are the ones presented in [21], where the case $D = 5$ was studied. Comparison with their numerical data shows that there is a very good agreement between our results obtained by using the WKB method and the exact numerical ones, and that the higher the WKB order is, the better the accuracy. It is known that the WKB method is accurate for modes with $\ell > n$; therefore, within the lower overtones, the worst (but still reasonable) precision will be for the fundamental scalar mode ($\ell = n = 0$): we have found $0.265\,391 - 0.497\,380i$ in 3rd WKB order, and $0.256\,429 - 0.391\,293i$ in 6th WKB order, while the numerical value is $0.273\,39 - 0.410\,91$, i.e. the relative error is about 4% for the real part and 2% for the imaginary part. For the fermionic ($k = 1$, $n = 0$) and electromagnetic ($\ell = 1$, $n = 0$) fundamental mode, the WKB method is expected to be rather accurate since $k, \ell > n$. Indeed, for the electromagnetic mode, for example, we have found $0.545\,243 - 0.331\,346i$ in 3rd WKB order, and $0.576\,508 - 0.313\,923i$ in 6th WKB order, while the numerical value is $0.576\,67 - 0.317\,49i$; therefore, the relative error is less then 0.01% for the real part, and about 0.2% for the imaginary part. For higher multipoles, a much better WKB accuracy is expected. As the reader will note, the two 6th order WKB values for the modes $k = n = 1$ and $\ell = n = 1$ for $D = 6$ are absent from Tables II and III: this is due to the fact that, for particular modes, the WKB method begins to show bad convergence as D starts taking large values.

One can find an analytical expression for QNMs in the limit of large multipole number ℓ, by making use of the formula (23) within first order and expanding in terms of $1/\ell$. In the eikonal approximation—as this approximation is called—the following formula for scalar and electro-

TABLE I. WKB values of the quasinormal frequencies for scalar field perturbations in the 3rd and 6th order beyond the eikonal approximation with $\ell \geq n$ for a D-dimensional Schwarzschild black hole projected on the brane.

$D = 5$	WKB3	WKB6	$D = 6$	WKB3	WKB6
$\ell = 0;\ n = 0;$	$0.265\,391 - 0.497\,380i$	$0.256\,429 - 0.391\,293i$	$\ell = 0;\ n = 0;$	$0.249\,904 - 0.793\,263i$	$0.146\,960 - 0.600\,541i$
$\ell = 1;\ n = 0;$	$0.722\,899 - 0.368\,853i$	$0.748\,461 - 0.371\,463i$	$\ell = 1;\ n = 0;$	$0.705\,383 - 0.527\,453i$	$0.834\,846 - 0.512\,377i$
$\ell = 1;\ n = 1;$	$0.535\,200 - 1.234\,129i$	$0.568\,185 - 1.214\,473i$	$\ell = 1;\ n = 1;$	$0.355\,372 - 1.918\,880i$	$0.392\,642 - 1.711\,230i$
$\ell = 2;\ n = 0;$	$1.243\,914 - 0.358\,055i$	$1.249\,839 - 0.358\,066i$	$\ell = 2;\ n = 0;$	$1.376\,420 - 0.499\,199i$	$1.393\,460 - 0.507\,541i$
$\ell = 2;\ n = 1;$	$1.099\,791 - 1.124\,086i$	$1.111\,651 - 1.121\,364i$	$\ell = 2;\ n = 1;$	$1.039\,578 - 1.636\,385i$	$1.088\,113 - 1.656\,560i$
$\ell = 2;\ n = 2;$	$0.887\,537 - 1.946\,290i$	$0.887\,876 - 2.018\,084i$	$\ell = 2;\ n = 2;$	$0.564\,026 - 2.898\,250i$	$0.568\,158 - 3.208\,780i$
$\ell = 3;\ n = 0;$	$1.747\,954 - 0.355\,789i$	$1.750\,048 - 0.355\,587i$	$\ell = 3;\ n = 0;$	$1.971\,510 - 0.497\,366i$	$1.978\,550 - 0.496\,292i$
$\ell = 3;\ n = 1;$	$1.642\,277 - 1.091\,913i$	$1.646\,819 - 1.090\,268i$	$\ell = 3;\ n = 1;$	$1.733\,260 - 1.551\,881i$	$1.752\,046 - 1.543\,178i$
$\ell = 3;\ n = 2;$	$1.468\,478 - 1.870\,707i$	$1.458\,460 - 1.895\,964i$	$\ell = 3;\ n = 2;$	$1.347\,778 - 2.703\,307i$	$1.317\,857 - 2.782\,190i$
$\ell = 3;\ n = 3;$	$1.246\,835 - 2.677\,609i$	$1.219\,431 - 2.814\,159i$	$\ell = 3;\ n = 3;$	$0.851\,976 - 3.917\,659i$	$0.742\,520 - 4.384\,462i$

TABLE II. WKB values of the quasinormal frequencies for Dirac field perturbations in the 3rd and 6th order beyond the eikonal approximation with $k \geq n$ for a D-dimensional Schwarzschild black hole projected on the brane.

$D = 5$	WKB3	WKB6	$D = 6$	WKB3	WKB6
$k = 1; n = 0;$	$0.373\,020 - 0.400\,822i$	$0.427\,813 - 0.324\,042i$	$k = 1; n = 0;$	$0.296\,822 - 0.633\,767i$	$0.389\,272 - 0.404\,875$
$k = 1; n = 1;$	$0.236\,229 - 1.299\,335i$	$0.199\,685 - 1.251\,460i$	$k = 1; n = 1;$	$0.086\,481 - 1.975\,351i$	$\cdots$
$k = 2; n = 0;$	$0.945\,819 - 0.355\,450i$	$0.973\,434 - 0.351\,309i$	$k = 2; n = 0;$	$1.000\,893 - 0.499\,552i$	$1.122\,648 - 0.454\,934i$
$k = 2; n = 1;$	$0.771\,922 - 1.163\,379i$	$0.806\,766 - 1.115\,347i$	$k = 2; n = 1;$	$0.664\,689 - 1.765\,862i$	$0.712\,367 - 1.523\,422i$
$k = 2; n = 2;$	$0.555\,975 - 2.029\,365i$	$0.580\,093 - 2.075\,602i$	$k = 2; n = 2;$	$0.280\,211 - 3.100\,380i$	$0.329\,359 - 3.257\,230i$
$k = 3; n = 0;$	$1.471\,906 - 0.353\,568i$	$1.479\,067 - 0.354\,610i$	$k = 3; n = 0;$	$1.641\,846 - 0.490\,566i$	$1.668\,661 - 0.502\,019i$
$k = 3; n = 1;$	$1.341\,192 - 1.101\,171i$	$1.359\,844 - 1.095\,934i$	$k = 3; n = 1;$	$1.334\,248 - 1.595\,761i$	$1.417\,715 - 1.561\,658i$
$k = 3; n = 2;$	$1.143\,877 - 1.905\,989i$	$1.152\,074 - 1.932\,798i$	$k = 3; n = 2;$	$0.913\,705 - 2.836\,118i$	$0.932\,631 - 2.876\,656i$
$k = 3; n = 3;$	$0.898\,975 - 2.738\,309i$	$0.906\,727 - 2.920\,396i$	$k = 3; n = 3;$	$0.392\,077 - 4.126\,275i$	$0.331\,583 - 4.842\,823i$

magnetic perturbations is valid:

$$\omega = \sqrt{\frac{r_0^{D-3} - r_H^{D-3}}{r_0^{D-1}}}\left[\ell + \frac{1}{2} - i\sqrt{D-3}\left(n + \frac{1}{2}\right)\right], \quad (24)$$

where $r_H = \mu^{1/(D-3)}$ is the black hole horizon radius, and r_0, as mentioned above, the value of the radial coordinate where the effective potential attains its maximum value. For scalar, Dirac, and electromagnetic perturbations, this is given by

$$r_0 = \left(\frac{D-1}{2}\right)^{\frac{1}{D-3}} r_H + O(1/\ell). \quad (25)$$

Note that, for electromagnetic perturbations, the above equation is an exact one, valid for any multipole number ℓ. An expression similar to Eq. (24) can be found also for Dirac perturbations, and has the form

$$\omega = \sqrt{\frac{r_0^{D-3} - r_H^{D-3}}{r_0^{D-1}}}\left[k - i\sqrt{D-3}\left(n + \frac{1}{2}\right)\right]. \quad (26)$$

One may easily note that the above formulas, valid for large multipole numbers, work well even for relatively small ℓ, being a good approximation already at $\ell = 4$.

By looking at our data, displayed in Tables I, II, and III, one may draw important conclusions for the dependence of the QN frequencies on the dimensionality of spacetime D, spin s of the particle, and multipole moment ℓ. Although the various SM fields are restricted to live on a four-dimensional brane, their QN behavior is significantly different from the one in a purely four-dimensional Schwarzschild background, and resembles more the one of higher-dimensional fields living in the bulk. As in the case of gravitons propagating in the higher-dimensional spacetime [22], the imaginary part of the QN frequencies for all types of brane-localized fields increase, as D also increases. As a result, the greater the number of hidden extra dimensions is, the greater the damping rate, and thus the shorter-lived the quasinormal ringing phase on the brane. The behavior of the real part of the QN frequencies is however less monotonic and seems to crucially depend on the values of the multipole moment ℓ and overtone number n. For $\ell, k > 2$, the fundamental ($n = 0$) and first ($n = 1$) overtones are characterized by an increasing real oscillation frequency, as the value of D increases, in agreement with similar results derived for gravitational QNMs in the bulk [22]. We expect this behavior to hold for arbitrarily large multipole numbers where the eikonal approximation becomes valid: Fig. 1 depicts the dependence of ω_{Re} and ω_{Im} as a function of D in the eikonal regime, with the increase in both parts being obvious. For $\ell, k \leq 2$, or $n \simeq \ell, k$ though, our data seem to indicate that the real

TABLE III. WKB values of the quasinormal frequencies for electromagnetic field perturbations in the 3rd and 6th order beyond the eikonal approximation with $\ell \geq n$ for a D-dimensional Schwarzschild black hole projected on the brane.

$D = 5$	WKB3	WKB6	$D = 6$	WKB3	WKB6
$\ell = 1; n = 0;$	$0.545\,243 - 0.331\,346i$	$0.576\,508 - 0.313\,923i$	$\ell = 1; n = 0;$	$0.482\,332 - 0.459\,270i$	$0.624\,699 - 0.303\,498i$
$\ell = 1; n = 1;$	$0.317\,482 - 1.135\,031i$	$0.339\,969 - 1.081\,171i$	$\ell = 1; n = 1;$	$0.035\,275 - 1.686\,996i$	$\cdots$
$\ell = 2; n = 0;$	$1.142\,703 - 0.343\,905i$	$1.148\,267 - 0.342\,292i$	$\ell = 2; n = 0;$	$1.244\,327 - 0.472\,984i$	$1.261\,845 - 0.461\,549i$
$\ell = 2; n = 1;$	$0.992\,174 - 1.082\,547i$	$1.001\,222 - 1.074\,150i$	$\ell = 2; n = 1;$	$0.917\,401 - 1.543\,831i$	$0.937\,130 - 1.486\,197i$
$\ell = 2; n = 2;$	$0.767\,162 - 1.877\,775i$	$0.755\,782 - 1.948\,901i$	$\ell = 2; n = 2;$	$0.437\,738 - 2.732\,445i$	$0.351\,770 - 2.942\,018i$
$\ell = 3; n = 0;$	$1.675\,991 - 0.348\,490i$	$1.677\,917 - 0.348\,103i$	$\ell = 3; n = 0;$	$1.874\,058 - 0.482\,782i$	$1.879\,429 - 0.480\,246i$
$\ell = 3; n = 1;$	$1.567\,818 - 1.070\,305i$	$1.571\,663 - 1.067\,999i$	$\ell = 3; n = 1;$	$1.637\,735 - 1.506\,514i$	$1.649\,296 - 1.490\,905i$
$\ell = 3; n = 2;$	$1.389\,311 - 1.835\,125i$	$1.376\,476 - 1.860\,555i$	$\ell = 3; n = 2;$	$1.252\,908 - 2.624\,888i$	$1.201\,152 - 2.690\,547i$
$\ell = 3; n = 3;$	$1.160\,459 - 2.628\,529i$	$1.126\,499 - 2.770\,443i$	$\ell = 3; n = 3;$	$0.755\,313 - 3.806\,577i$	$0.604\,352 - 4.260\,917i$

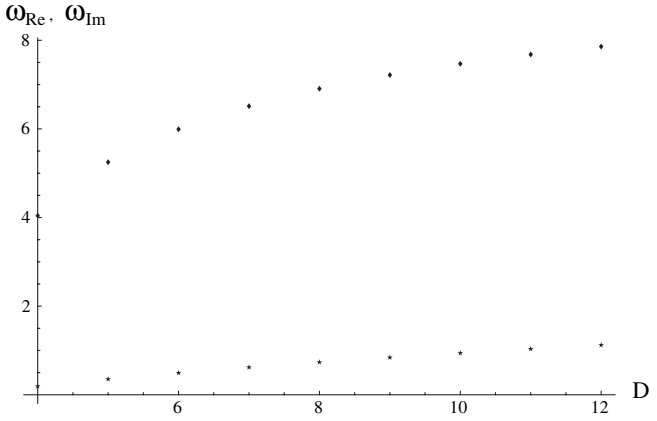

FIG. 1. Dependence of real (diamond) and imaginary (star) parts of quasinormal modes on spacetime dimensionality D in the eikonal approximation; for each D, we have chosen $\ell = 10$ and set $r_H = 1$.

part of the QN frequency tends to decrease with the total number of dimensions, with the only exceptions to this rule being the scalar and electromagnetic fundamental mode ($n = 0$) for $\ell = 1$. As nevertheless noted previously, the accuracy of our calculation decreases exactly in this regime; therefore, this result should be taken with caution and confirmed by numerical analysis.

Turning to the dependence of the QNM frequencies on the spin of the particle, let us consider the fundamental modes of all three types of SM fields that correspond to the lowest possible value of the multipole number in each case. Within the 6th order WKB approximation, we obtained: $\omega_{n=0} = 0.256\,43–0.391\,29i$ for scalar ($\ell = 0$), $\omega_{n=0} = 0.427\,81–0.324\,04i$ for Dirac ($k = 1$), and $\omega_{n=0} = 0.576\,51–0.313\,92i$ for gauge fields ($\ell = 1$). Therefore, among the lowest fundamental modes, the greater the spin of the field is, the greater the ω_{Re}, and the smaller the ω_{Im}. As a result, fields with higher spin will decay slower and will dominate during the "final ring-down" stage. To this respect, the brane-localized fields behave in a similar way to purely four-dimensional ones [3]. In contrast, in studying gravitational perturbations in the bulk, it was found that an increasing spin-weight led again to the enhancement of the real frequency but to the increase of the damping rate as well [22]. Among the lowest three fundamental modes mentioned above, the field with the higher spin ($s = 1$) has also the largest ratio $|\omega_{\mathrm{Re}}/\omega_{\mathrm{Im}}|$, known as the quality factor of the oscillator, a result that renders this mode the best oscillator of all three in the vicinity of the projected-on-the-brane black hole. However, if we look at the fundamental modes corresponding to higher values of the multipole number, one may see that, for fixed ℓ, it is instead the scalar field that is the better oscillator of all three species.

Finally, for fixed dimensionality of spacetime and spin of the particle, the various QN frequencies still depend on the multipole number ℓ. A simple inspection of our data shows that, for brane-localized fields, the real oscillatory part increases with ℓ, for all species of fields and values of D. The imaginary part of the frequency is decreasing for scalar fields and increasing for fermions and gauge fields, however in all cases it soon approaches a constant value. This is in agreement with Eqs. (24) and (26), from where we may see that, in the high frequency approximation ($\ell \to \infty$), the real part of each mode is proportional to the multipole number ℓ, while the damping rate approaches a constant value that depends solely on the fundamental parameters of the gravitational system such as r_H, r_0, and D.

IV. CHARGED NONROTATING BLACK HOLE: WKB VALUES OF BRANE QNMS

In this case, the metric function $h(r)$, that describes the projected-on-the-brane Reissner-Nordström black hole line element, is given by Eq. (5). The corresponding effective potentials V_s for the various SM fields propagating on the brane are again determined by the formulas in Eqs. (18)–(21), and, as before, have the form of positive-definite potential barriers. As a result, the WKB method can be consistently applied also in this case.

The quasinormal modes of a four-dimensional Reissner-Nordström black hole were investigated in [23] within the WKB approximation, and in [24] with the help of the Frobenius method. Quasinormal modes of more general, or alternative, solutions for charged black holes also were considered in the literature: $(D > 4)$-dimensional Reissner-Nordström black holes [22], dilaton black holes [25], and Born-Infeld black holes [26]. In all the aforementioned works, one common feature was found to emerge concerning the QNMs of charged black holes: the damping rate was monotonically increasing as a function of the charge Q, until a critical value $Q \approx 0.7 - 0.8Q_{\mathrm{ext}}$ was reached; after this point, the behavior of the damping rate changed to sharply decreasing. Thereby, ω_{Im} as a function of Q had a maximum somewhere near the value $Q \approx 0.7$–$0.8Q_{\mathrm{ext}}$, where $Q_{\mathrm{ext}} = \mu/2$ is the value of the charge that corresponds to an extreme charged black hole with a degenerate horizon.

In Figs. 2 and 3 and Table IV, we display an indicative sample of our results, derived by using the 6th order beyond the eikonal approximation WKB method; these correspond to the fundamental modes ($n = 0$) for scalars, fermions, and gauge fields, for the multipole number values $\ell = 2$ and $\ell = 1$, respectively. For simplicity, the mass parameter and therefore the extremal value of the charge have been fixed to the values $\mu = 1$ and $Q_{\mathrm{ext}} = 0.5$, respectively. For a given value of the charge Q, the dependence of the QNMs on D and spin s remains the same as in the neutral case; therefore, we will not comment further on this dependence here. We will instead focus our attention to the dependence of the QN frequency solely on the charge of the black hole.

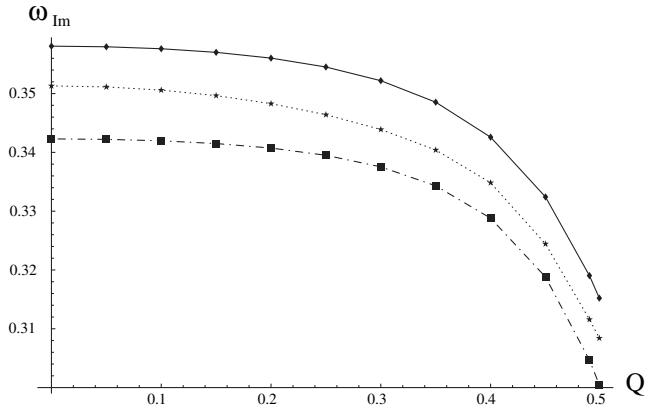

FIG. 2. Dependence of imaginary part of quasinormal modes on charge Q for $\ell = 2$; $r_H = 1$, $D = 5$. Scalar (diamond), Dirac (star), and vector (box) perturbations.

According to our results, the quasinormal modes of particles living in a charged black hole background projected on the brane have one, very distinctive feature compared to the previously studied Reissner-Nordström cases: the characteristic maximum of the damping rate as a function of the charge is absent. Indeed, as one may see in Fig. 2, the damping rate of the $\ell = 2$ fundamental modes of all species of fields is a monotonically decreasing function of the charge Q. The same behavior was found for the fundamental modes of all species corresponding to higher multipole numbers, $\ell > 2$. The absence of the aforementioned maximum is not a feature unseen before; it has been observed recently for D-dimensional black holes in Gauss-Bonnet theory [27]. The real oscillatory part of the QN frequency on the other hand was found to be monotonically increasing, as a function of Q, for all species of particles, and its exact dependence for the case $\ell = 2$ is depicted in Fig. 3.

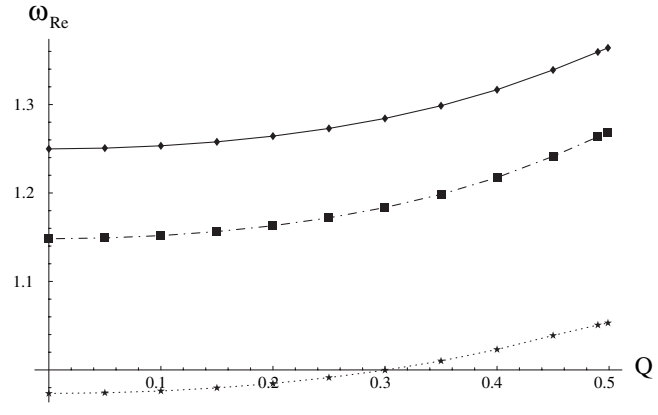

FIG. 3. Dependence of real part of quasinormal modes on charge Q for $\ell = 2$; $r_H = 1$, $D = 5$. Scalar (diamond), vector (box), and Dirac (star) perturbations.

TABLE IV. WKB values in 6th order beyond the eikonal approximation for quasinormal frequencies of brane-localized fields, for $D = 5$ and $D = 6$ Reissner-Nordström black holes; $\ell = 1$, $n = 0$.

s	Q	$D = 5$	$D = 6$
0	0.05	$0.749\,152 - 0.371\,256i$	$0.835\,852 - 0.511\,642i$
0	0.15	$0.754\,757 - 0.369\,605i$	$0.843\,518 - 0.506\,642i$
0	0.25	$0.766\,514 - 0.366\,119i$	$0.858\,076 - 0.499\,811i$
0	0.35	$0.786\,714 - 0.358\,488i$	$0.887\,353 - 0.484\,023i$
0	0.45	$0.818\,792 - 0.334\,299i$	$0.934\,330 - 0.425\,248i$
0	0.499	$0.830\,394 - 0.313\,416i$	$0.935\,737 - 0.396\,232i$
1/2	0.05	$0.428\,119 - 0.323\,953i$	$0.389\,386 - 0.403\,475i$
1/2	0.15	$0.430\,879 - 0.322\,740i$	$0.392\,510 - 0.388\,419i$
1/2	0.25	$0.438\,019 - 0.318\,018i$	$0.409\,388 - 0.346\,311i$
1/2	0.35	$0.447\,564 - 0.314\,646i$	$0.390\,580 - 0.382\,414i$
1/2	0.45	$0.458\,170 - 0.320\,913i$	$0.419\,673 - 0.437\,986i$
1/2	0.499	$0.450\,377 - 0.290\,551i$	$0.355\,861 - 0.374\,075i$
1	0.05	$0.577\,071 - 0.314\,252i$	$0.625\,394 - 0.305\,570i$
1	0.15	$0.581\,787 - 0.316\,804i$	$0.632\,436 - 0.321\,188i$
1	0.25	$0.592\,555 - 0.321\,297i$	$0.655\,043 - 0.345\,745i$
1	0.35	$0.613\,317 - 0.324\,651i$	$0.712\,217 - 0.358\,226i$
1	0.45	$0.652\,107 - 0.311\,345i$	$0.811\,198 - 0.319\,470i$
1	0.499	$0.668\,226 - 0.289\,308i$	$0.832\,820 - 0.291\,253i$

As in the previous subsection, the fundamental modes of some species of fields for the multipole number $\ell = 1$ offer an exception to the aforementioned rule. In Table IV, we display these modes for all species of fields of the standard model. While the $\ell = 1$ fundamental mode of scalar fields follows the behavior displayed in Figs. 2 and 3 both for the imaginary and real part of the QN frequency, the one of fermions and gauge bosons deviate by exhibiting a nonmonotonic behavior. In the case of fermions, the imaginary part of the QN frequency does initially decrease with the charge Q, as the rule dictates; however, for higher values of Q, it goes through a maximum value before decreasing again; similarly, its real part starts increasing as expected but again, after a critical point is reached, it starts decreasing. In the case of gauge bosons, the real part of the $\ell = 1$ fundamental mode does indeed follow the pattern shown in Fig. 3; however, its imaginary part seems to follow instead the traditional Reissner-Nordström frequency behavior by initially increasing with Q and then decreasing. The behavior described above holds both for $D = 5$ and $D = 6$, with the increase in the dimensionality of spacetime enhancing the height of the various maxima points.

Let us note at this point that, throughout this analysis, we consider minimally-coupled fields propagating in a given black hole background projected on the brane. As a result, we do not take into account the interaction of the spin-1 propagating particle with the electromagnetic field of the black hole background. In a more realistic description, the electromagnetic perturbations will induce gravitational ones and vice verca, and the quasinormal spectrum of

vector perturbations may be considerably different from the one described here.

As in the case of a neutral Schwarzschild black hole, an expression may be derived that describes the QN frequency in the eikonal approximation, i.e. in the limit of large multipole number. By making use of the first order WKB approximation, one can obtain, in the eikonal regime $\ell \to \infty$, the following formula

$$\omega = \sqrt{\frac{Q^2 - \mu r_0^{D-3} + r_0^{2D-6}}{r_0^{2D-4}}}\left[\ell + \frac{1}{2} - iC\left(n + \frac{1}{2}\right)\right], \tag{27}$$

for scalar and vector perturbations, and

$$\omega = \sqrt{\frac{Q^2 - \mu r_0^{D-3} + r_0^{2D-6}}{r_0^{2D-4}}}\left[k - iC\left(n + \frac{1}{2}\right)\right], \tag{28}$$

for Dirac perturbations. As before, r_0 denotes the value of the radial coordinate that corresponds to the maximum of the effective potential, which is now given by

$$r_0 = \left[\frac{(D-1)\mu + \sqrt{(D-1)^2\mu^2 - 16(D-2)Q^2}}{4}\right]^{1/(D-3)}, \tag{29}$$

also in the limit $\ell \to \infty$. In the above equations, C is a rather cumbersome constant depending on the black hole parameters μ and Q and on the spacetime dimensionality D. When $Q = 0$, the above formulas reduce to Eqs. (24)–(26) for a neutral black hole. One may clearly see that, even for a nonvanishing value of Q, the real part of the QN frequency increases proportionally to the multipole number, while the imaginary part, and thus the damping rate, is determined through C by the fundamental parameters of the problem.

V. SCHWARZSCHILD-DE SITTER BLACK HOLE: WKB VALUES OF BRANE QNMS

We now turn to the case of a D-dimensional Schwarzschild-de Sitter (SdS) black hole projected onto a four-dimensional brane. The corresponding line element is defined in terms of the metric function $h(r)$ given in Eq. (6) with a positive cosmological constant, $\Lambda > 0$. This gravitational background is characterized by two horizons: the black hole event horizon r_H and the cosmological horizon r_c. The effective potentials (18)–(21), again, take the form of a potential barrier that vanishes at both horizons. We can, therefore, once again apply consistently the WKB method.

In Table V, we display our results for the QNM frequencies for scalar, Dirac, and electromagnetic perturbations propagating in the vicinity of a projected-on-the-brane SdS black hole. The data correspond to the fundamental modes for the value $\ell = 1$ of the multipole number, and for the dimensionalities $D = 5$ and $D = 6$. The value of the cosmological constant is parameterized in terms of its extreme value $\Lambda_{\rm ext}$ that corresponds to the degenerate case where the black hole and cosmological horizon coincide. This maximal value of Λ is defined through the relation:

TABLE V. WKB values in 6th order beyond the eikonal approximation for quasinormal frequencies of brane-localized fields, for $D = 5$ and $D = 6$ SdS black holes; $\ell = 1$, $n = 0$.

s	$\Lambda/\Lambda_{\rm ext}$	$D = 5$	$D = 6$
0	0.1	0.702 057–0.358 774i	0.775 357–0.504 744i
0	0.4	0.545 649–0.305565i	0.588 540–0.445 438i
0	0.6	0.424 729–0.251 384i	0.450 599–0.369 360i
0	0.8	0.282 756–0.172 529i	0.291 411–0.252 903i
0	0.99	0.0613 94–0.035 506i	0.064 318–0.049 5684i
1/2	0.1	0.413 557–0.305 111i	0.391 439–0.375 808i
1/2	0.4	0.357 933–0.246 785i	0.376 180–0.298 955i
1/2	0.6	0.303 241–0.204 146i	0.335 594–0.252 227i
1/2	0.8	0.201 820–0.162 479i	0.205 018–0.234 865i
1/2	0.99	0.048 920–0.035 784i	0.054 487–0.050 475i
1	0.1	0.550 719–0.300 547i	0.591 162–0.306 145i
1	0.4	0.459 051–0.253 351i	0.483 397–0.295 120i
1	0.6	0.379 611–0.212 105i	0.397 151–0.265 749i
1	0.8	0.271 415–0.154 087i	0.283 191–0.205 254i
1	0.99	0.061 232–0.0353 454i	0.063 908–0.049 419i

$$\mu^2 = \frac{4(D-3)^{D-3}}{(D-1)^{D-1}}\left(\frac{(D-1)(D-2)}{2\kappa_D^2\Lambda_{\rm ext}}\right)^{D-3}. \tag{30}$$

The behavior of the QN frequencies of the various species of brane-localized fields does not yield any surprises in regard with their dependence on the cosmological constant. Similarly to the behavior exhibited by fields in the vicinity of a purely four-dimensional SdS spacetime [3] or by gravitational fields living in a D-dimensional SdS spacetime [22], both the real and imaginary parts of the QN frequency are decreasing as the value of the cosmological constant increases. This decrease is observed, and has the same magnitude, for all species of fields: as Λ ranges from zero to its maximum value $\Lambda_{\rm ext}$, all fields undergo a suppression of their QN frequency by approximately 90%. For any given value of Λ, an increase in the dimensionality of spacetime results, as in the case of QNMs of bulk gravitons, to an increase of the value of both $\omega_{\rm Re}$ and $\omega_{\rm Im}$. Nevertheless, the relative suppression of ω with Λ remains the same.

As it is well known, in the regime of near extremal values of Λ, the effective potential approaches the Poschl-Teller potential [28] for which there is an exact analytical solution. Therefore, the exact formula for QNMs in the extremal limit is

$$\frac{\omega}{k_H} = \sqrt{\frac{\ell(\ell+1)(r_c - r_H)}{2k_H r_H^2} - \frac{1}{4}} - i\left(n + \frac{1}{2}\right), \tag{31}$$

for scalar and electromagnetic perturbations, and

$$\frac{\omega}{k_H} = \sqrt{\frac{k^2(r_c - r_H)}{2k_H r_H^2} - \frac{1}{4}} - i\left(n + \frac{1}{2}\right), \tag{32}$$

for Dirac perturbations. Here, the radii of the event and cosmological horizon are approximated by the formulas:

$$r_H \approx \sqrt{\frac{(D-1)(D-2)}{2\kappa_D^2 \Lambda}}\left(\sqrt{\frac{D-3}{D-1}} - \frac{\delta}{D-1}\right), \tag{33}$$

$$r_c \approx \sqrt{\frac{(D-1)(D-2)}{2\kappa_D^2 \Lambda}}\left(\sqrt{\frac{D-3}{D-1}} + \frac{\delta}{D-1}\right), \tag{34}$$

respectively, where

$$\delta = \sqrt{1 - \frac{\mu^2 (D-1)^{D-1}}{4(\frac{(D-1)(D-2)}{2\kappa_D^2 \Lambda})^{D-3}(D-3)^{D-3}}}. \tag{35}$$

Finally, the surface gravity k_H at the event horizon is given by the formula

$$k_H = \frac{1}{2}\frac{dh(r)}{dr^*}|_{r=r_H}. \tag{36}$$

As we can see from the above formulas, in the extremal limit, fields of different spin decay with exactly the same rate. Indeed, from the entries of Table V, one can see that, despite its initially different values, ω_{Im} reduces to almost the same value for all species of fields when $\Lambda = 0.99\Lambda_{\mathrm{ext}}$. Note that the same behavior is observed in the QNM spectrum for ordinary four-dimensional SdS black holes [29] and is therefore not an unexpected property of the QN spectrum of brane-localized fields.

In the regime of large multipole numbers ℓ, the value of the radial coordinate $r = r_0$, at which the effective potential has a maximum, is again expressed by Eq. (25) for fields of any spin. Using the first order WKB formula, one can find

$$\omega = \sqrt{\frac{1}{r_0^2} - \frac{\mu}{r_0^{D-1}} - \frac{2\kappa_D^2 \Lambda}{(D-1)(D-2)}}\left[\ell + \frac{1}{2} + iC\left(n + \frac{1}{2}\right)\right], \tag{37}$$

for scalar and electromagnetic perturbations, and

$$\omega = \sqrt{\frac{1}{r_0^2} - \frac{\mu}{r_0^{D-1}} - \frac{2\kappa_D^2 \Lambda}{(D-1)(D-2)}}\left[k + iC\left(n + \frac{1}{2}\right)\right], \tag{38}$$

for Dirac perturbations. When $D = 4$, the above formulas go over to the ones for SdS black holes presented in [29].

VI. SCHWARZSCHILD-ANTI–DE SITTER BLACK HOLE: QNMS OF BRANE FIELDS

A great interest in quasinormal modes for asymptotically anti–de Sitter (AdS) black holes was stipulated the last 5 years after the observation was made, first in [30], that quasinormal modes of classical $(D + 1)$-dimensional asymptotically AdS black holes should coincide with poles of the retarded Green function in the dual conformal field theory (CFT) at finite temperature in D dimensions in the limit of strong coupling. In this context, the black hole temperature corresponds to the temperature in the dual thermal field theory. Therefore, by making use of this correspondence, one can investigate different thermal phenomena in the limit of strong coupling in CFT, such as dispersion relations and the hydrodynamic limit of CFT [31].

Assuming that the background in the bulk coincides with the one of a Schwarzschild-anti–de Sitter (SAdS) black hole, the projected-on-the-brane line element will be described once again by Eq. (7), where $h(r)$ is given in Eq. (6) with the cosmological constant now taking negative values, $\Lambda < 0$. For later use, we define the "effective" anti–de Sitter radius R as

$$R = \sqrt{\frac{(D-1)(D-2)}{2\kappa_D^2 |\Lambda|}}. \tag{39}$$

In the case of an SAdS background, the effective potentials (18)–(21) vanish at the black hole horizon but are divergent at infinity, and therefore Dirichlet boundary conditions, demanding the vanishing of the fields themselves at infinity, are physically motivated. For perturbations of scalar fields, the application of the Dirichlet boundary conditions poses no problem, as these are also required by the AdS/CFT correspondence. However, for fields of higher spin, one needs to impose the boundary conditions not on the wave function Ψ of the field, but on some alternative function that has the correct interpretation in the context of the dual CFT [31]. The form of the correct boundary conditions for higher-spin fields in an asymptotically AdS spacetime is a controversial, and still open, question. Since our interest in the AdS case is motivated mainly by the AdS/CFT interpretation of the quasinormal modes, here we limit our discussion to the case of scalar fields for which the correct boundary conditions are known.

In order to find the quasinormal modes for scalar field perturbations in the projected-on-the-brane SAdS background, we shall apply the Horowitz-Hubeny method [30]. As this method is described in many papers, here we will outline only its main points. Near the event horizon, one can expand the wave function $\Psi(r)$ of the field in the following way:

$$\Psi(x) = \sum_{m=0}^{\infty} a_m (x - x_H)^m, \qquad x_H = 1/r_H. \tag{40}$$

Here, r_H is the largest of the zeros of the metric function $h(r)$, that corresponds to the black hole horizon radius. On the other hand, at infinity, the Dirichlet boundary conditions, that we will use here, dictate that

$$|\Psi(r = +\infty)| \equiv |\Psi(x = 0)| = 0. \tag{41}$$

The method amounts to solving the above equation, whose roots will then give us the corresponding quasinormal frequencies ω. To this end, we need to truncate the sum (40) at some large $m = N$ and make sure that the roots of Eq. (41) still converge for higher values of m. Note that the larger the dimensionality D is, the larger the truncation number N needs to be. In addition, for small black holes and high overtones we need a very large N in order to find the QN modes with a good accuracy. Thus, for instance, for $r_H \approx 0.6$ and $D = 6$, $N \approx 10^4$.

The properties of the quasinormal spectrum for asymptotically AdS black holes strongly depend on the size of the black hole relative to the AdS radius. Thus, QN spectra of large ($r_H \gg R$), intermediate ($r_H \approx R$), and small ($r_H \ll R$) black holes are totally different. QNMs of large AdS black holes are proportional to the black hole radius and therefore proportional to the temperature of the black hole [30]. In the regime of intermediate black holes, this proportionality is broken [30], and, for small AdS black holes, QNMs reduce to the normal modes of the AdS spacetime when a black hole radius goes to zero [32]. At high overtones, the quasinormal spectrum becomes equidistant, with a spacing which is independent of the multipole number and spin of the field being perturbed [33]. Below, we shall show that the above properties also hold for a higher-dimensional, asymptotically AdS black hole projected on the brane.

The fundamental quasinormal frequencies for scalar field perturbations ($\ell = 0, n = 0$) in the vicinity of a SAdS black hole projected on the brane, are shown in Table VI, for the cases $D = 5$, 6, and 7. The black hole horizon radius is taken to cover the regime from a fraction of the AdS radius to a hundred times larger than R. From the displayed data, one may easily see that the QN frequency increases as the black hole horizon increases, and that, for $r_H \gg R$, ω is indeed proportional to r_H. The asymptotic regime of high damping begins at relatively small overtone numbers, i.e. at $n \approx 10$. In Table VII, we display the first nine overtones for a projected-on-the-brane SAdS black hole with $r_H = 100R$, from where we may see that the quasinormal spectrum very quickly becomes equidistant with a spacing that depends only on the dimensionality of spacetime D and the black hole horizon r_H. From the numerical data of Table VII, we may deduce the spacing for both the real and imaginary part of the QN frequency, that come out to be

$$\omega_{n+1} - \omega_n \approx 2(1 + i) r_H, \qquad D = 5, \tag{42}$$

$$\omega_{n+1} - \omega_n \approx (2.4 + 1.7i) r_H, \qquad D = 6. \tag{43}$$

Let us consider next the limit of a very small black hole radius. From Ref. [32] one can learn that the QNMs of an asymptotically AdS black hole approaches its pure AdS values (normal modes). The normal modes for scalar fields in an AdS spacetime can be found analytically. For the case of a field propagating on a brane, that is embedded in a pure AdS spacetime, the metric function takes the form

$$h(r) = 1 - \frac{2\kappa_D^2 \Lambda r^2}{(D-1)(D-2)}, \qquad \Lambda < 0, \tag{44}$$

and describes an effective four-dimensional anti–de Sitter spacetime with a rescaled cosmological constant: $\Lambda \to 6\Lambda/(D-1)(D-2)$. Therefore, the normal modes for brane-localized scalar field perturbations can follow immediately from the corresponding analysis of the purely four-dimensional case [33] and are given by

$$\omega_{\text{scalar}} = \sqrt{\frac{2\kappa_D^2 |\Lambda|}{(D-1)(D-2)}}(2n + \ell + 3). \tag{45}$$

For instance, for the particular case of $n = 0$ and $D = 5$, the above formula leads to the result: $\omega_{n=0} \approx 3$. Then, from the entries of Table VI, one may clearly see that, as the black hole radius decreases, the QN frequency asymptotes to the same value. Thus, the QN modes of scalar fields, in the vicinity of a very small asymptotically AdS

TABLE VI. Fundamental quasinormal frequencies ($\ell = 0$, $n = 0$) for scalar field perturbations for a Schwarzschild-anti–de Sitter black hole; $D = 5$, 6, and 7.

r_H	$D = 5$	$D = 6$	$D = 7$
100 R	262.029 34–230.209 13i	299.444 02–200.49039i	320.321 24–179.053 96i
50 R	131.032 12–115.103 40i	149.743 31–100.242 19i	160.185 52–89.521 88i
10 R	26.335 89–23.008 14i	30.084 65–20.029 29i	32.173 41–17.877 98i
5 R	13.368 30–11.484 60i	15.252 71–9.985 09i	16.301 17–8.908 85i
1 R	3.7449–2.1871i	4.170 56–1.846 84i	4.395 42–1.625 36i
0.8 R	3.4051–1.7056i	3.76 193–1.424 08i	3.946 02–1.247 88i
0.6 R	3.1239–1.2168i	3.41 142–0.998 47i	3.553 67–0.870 43i

TABLE VII. Higher overtones for scalar field perturbations of large ($r_H = 100R$) SAdS black hole; $D = 5, 6$; $\ell = 0$.

n	$D = 5$	$D = 6$
1	465.017 79−431.643 99i	541.129 45−374.619 83i
2	665.992 15−632.022 15i	780.161 18−547.738 31i
3	866.460 20−832.184 57i	1018.545 15−720.654 33i
4	1066.731 87−1032.272 06i	1256.674 21−893.495 63i
5	1266.908 74−1232.325 73i	1494.678 36−1066.301 65i
6	1467.033 27−1432.361 58i	1732.612 61−1239.088 44i
7	1667.126 14−1632.386 99i	1970.504 06−1411.863 65i
8	1867.198 51−1832.405 82i	2208.36 754−1584.631 41i
9	2067.25 695−2032.420 267i	2446.211 80−1757.394 10i

black hole projected on the brane, approach indeed the normal modes of the pure AdS spacetime.

In Fig. 4, we depict the dependence of the QNM frequency spectrum on the multipole number ℓ. In contrast to what happens in the asymptotically flat case, where the imaginary part of the QN frequency was approaching a constant value in the limit $\ell \to \infty$, in the case of a SAdS black hole, the damping rate is decreasing when ℓ is growing, therefore higher multipoles should decay more slowly. Yet, as was mentioned in [30], this does not pose a problem for AdS/CFT correspondence since a decomposition according to multipole numbers can be done in the dual CFT as well.

Finally, another deviation—from the behavior noted in the previously studied cases—is observed here, this time in respect to the dependence of the QN spectrum on the dimensionality of spacetime. According to our results, in the case of a projected-on-the-brane SAdS black hole, when the number of hidden, transverse dimensions increases, the imaginary part of the QN frequencies is decreasing, while the real part of ω is increasing. We remind the reader that in the case of asymptotically flat or de Sitter black holes, both ω_{Re} and ω_{Im} grow when D is increasing (see, for example, Fig. 1).

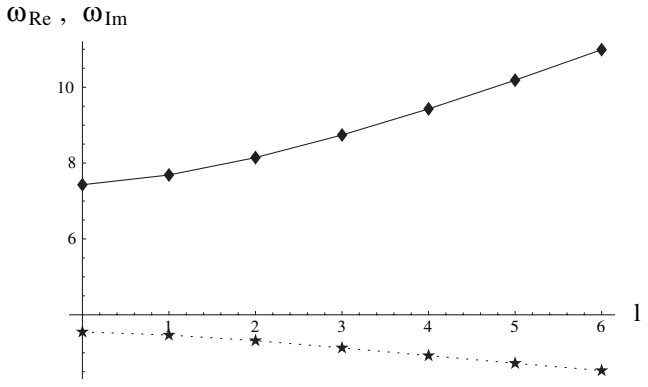

FIG. 4. Dependence of the real (diamond) and imaginary (star) part of QNMs on multipole number ℓ, for $n = 0$, $r_H = 1$, and $D = 6$. Scalar field perturbations of SAdS black hole.

VII. CONCLUSIONS

The theories postulating the existence of extra, compact spacelike dimensions have opened the way for low-scale gravitational theories and the observation of strong gravitational phenomena such as the creation of tiny, higher-dimensional black holes in the controlled environment of a ground-based particle accelerator. Standard model fields, that are restricted to live on the four-dimensional brane and happen to propagate in the vicinity of such a black hole, will feel only the projected-on-the-brane black hole background. In such a situation, the observation of their QN frequencies may be highly more likely to take place than the one for the diligently pursued, but up to now elusive, gravitons. Such a detection will provide not only evidence for the existence of the black holes themselves, but also information on the fundamental parameters of the higher-dimensional theory.

In this work, we have investigated a variety of spherically-symmetric D-dimensional black hole backgrounds, that are then projected onto the four-dimensional brane. The induced-on-the-brane backgrounds depend on a single metric function $h(r)$, that carries a signature of the parameters of the D-dimensional theory, such as the dimensionality D, charge Q, and cosmological constant Λ. The same function characterizes the form of the effective potentials felt by the scalars, fermions, and gauge bosons propagating in the brane background. In three of the cases studied (Schwarzschild, Reissner-Nordström, and Schwarzschild-de Sitter), the effective potentials had the form of positive-definite barriers, a result that allowed us to use the WKB method to derive the QN spectrum in the 6th order beyond the eikonal approximation. In the fourth case (Schwarzschild-anti−de Sitter), the effective potential diverged at infinity, and the Horowitz-Hubeny method was used instead.

In the case of a Schwarzschild black hole background, the QN spectrum of all SM fields was computed for various values of the dimensionality of spacetime D and multipole number ℓ. It was found that, as the number of hidden, extra dimensions increased, the imaginary part of the QN fre-

quency for all species increased as well, thus making the ring-down phase on the brane shorter. The real part of the QN frequency was also found to be D dependent and to predominantly increase with D, although particular modes with $\ell \simeq n$ may deviate from this behavior. In respect to the dependence on the spin, fields with higher spin were found to damp with a slower rate and thus to survive longer.

If a charge Q is present in the bulk background, the QN frequency spectrum is found to significantly deviate from the one of purely four-dimensional ones and to resemble more the one in the vicinity of a D-dimensional Gauss-Bonnet black hole: an increase in the charge of the black hole was found to lead to a monotonically decreasing behavior for the imaginary part of the QN frequency—and thus to a longer ring-down phase—and to a monotonically increasing behavior for the real part, rendering all SM fields much better oscillators than in the neutral case.

When a positive cosmological constant is turned on in the bulk, the resulting QN spectrum of the SM fields on the brane does not yield any surprises. As Λ increases, both the real and imaginary part of the QN frequency are suppressed, and for $\Lambda = \Lambda_{\text{ext}}$, the suppression reaches the magnitude of 90%. The number of dimensions enhances again the individual values of ω_{Re} and ω_{Im}, however the relative suppression as Λ varies comes out to be only mildly D dependent. In the extreme limit, the feature of fields with different spin decaying with almost the same rate is observed also in the present case of brane-localized fields in an effective SdS background.

In the case of a negative cosmological constant being present in the bulk, the spectrum of QN frequencies was shown to depend on the ratio of the black hole horizon to the AdS radius, similarly to the case of purely four-dimensional or D-dimensional SAdS backgrounds. For large black holes, the QN spectrum comes out to be proportional to r_H, and to become equidistant for the higher overtones. In the opposite limit of a very small black hole, the QN frequencies approach the normal modes of the projected-on-the-brane AdS spacetime.

Summarizing our results, we may say that the existence of extra dimensions affects the QNM spectrum of fields living on the brane both in a direct and an indirect way. In all the cases studied here, an increase in the number of transverse-to-the-brane dimensions causes a significant increase in the imaginary part of all fields, thus directly affecting the damping rate of the field perturbations on the brane. Additional features, such as the distance in the frequency spacing between successive quasinormal modes in the SAdS spacetime, or asymptotic values of QN frequencies in various limits and backgrounds, also depend explicitly on the total number of dimensions D. In an indirect way, the localization of fields on a brane embedded in a higher-dimensional black hole background leads to a deviation from the behavior observed either in the purely four-dimensional or in a purely D-dimensional case: the monotonic behavior of the QN spectrum as a function of the charge Q, for the majority of the modes, is an indicative example of this.

In this work, we have restricted our analysis to the study of spherically symmetric D-dimensional black hole backgrounds projected on the brane. The study of axially symmetric, rotating black hole backgrounds has already been initiated and we hope to report our results soon in a follow-up article. In addition, here we were limited by the consideration of quasinormal spectra for only massless fields, yet, as was shown in [34] for scalars, and in [35] for vector fields, the mass term can change the lower modes of the spectrum considerably, leaving unaffected the high damping limit of the spectrum—the study of the effect of the mass term on the QN spectrum of brane-localized fields in various backgrounds is also among our future plans.

ACKNOWLEDGMENTS

P. K. acknowledges financial support from the U. K. Particle Physics and Astronomy Research Council Grant No. PPA/A/S/2002/00350. The work of R. K. was supported by *Fundação de Amparo à Pesquisa do Estado de São Paulo (FAPESP)*, Brazil.

[1] H. P. Nollert, Classical Quantum Gravity **16**, R159 (1999).
[2] K. D. Kokkotas and B. G. Schmidt, Living Rev. Relativity **2**, 2 (1999).
[3] P. R. Brady, C. M. Chambers, W. G. Laarakkers, and E. Poisson, Phys. Rev. D **60**, 064003 (1999); B. Wang, E. Abdalla, and R. B. Mann, Phys. Rev. D **65**, 084006 (2002); V. Suneeta, Phys. Rev. D **68**, 024020 (2003); A. Zhidenko, gr-qc/0510039; J. x. Tian, Y. x. Gui, G. h. Guo, Y. Lv, S. h. Zhang, and W. Wang, Gen. Relativ. Gravit. **35**, 1473 (2003); C. Molina, D. Giugno, E. Abdalla, and A. Saa, Phys. Rev. D **69**, 104013 (2004); E. Abdalla, R. A. Konoplya, and C. Molina, Phys. Rev. D **72**, 084006 (2005); T. R. Choudhury and T. Padmanabhan, Phys. Rev. D **69**, 064033 (2004); M. Giammatteo and I. G. Moss, Classical Quantum Gravity **22**, 1803 (2005); V. Cardoso, J. Natario, and R. Schiappa, J. Math. Phys. (N.Y.) **45**, 4698 (2004).
[4] N. Arkani-Hamed, S. Dimopoulos, and G. R. Dvali, Phys. Lett. B **429**, 263 (1998); Phys. Rev. D **59**, 086004 (1999); I. Antoniadis, N. Arkani-Hamed, S. Dimopoulos, and G. R. Dvali, Phys. Lett. B **436**, 257 (1998).
[5] L. Randall and R. Sundrum, Phys. Rev. Lett. **83**, 3370 (1999); Phys. Rev. Lett. **83**, 4690 (1999).
[6] F. R. Tangherlini, Nuovo Cimento **27**, 636 (1963).

[7] R. C. Myers and M. J. Perry, Ann. Phys. (N.Y.) **172**, 304 (1986).
[8] G. T. Horowitz and V. E. Hubeny, Phys. Rev. D **62**, 024027 (2000); V. Cardoso, O. J. C. Dias, and J. P. S. Lemos, Phys. Rev. D **67**, 064026 (2003); C. Molina, Phys. Rev. D **68**, 064007 (2003); V. Cardoso, S. Yoshida, O. J. C. Dias, and J. P. S. Lemos, Phys. Rev. D **68**, 061503 (2003); V. Cardoso, J. P. S. Lemos, and S. Yoshida, J. High Energy Phys. 12 (2003) 041; Phys. Rev. D **69**, 044004 (2004); G. Siopsis, Phys. Lett. B **590**, 105 (2004); V. Cardoso, O. J. C. Dias, and J. P. S. Lemos, Phys. Rev. D **70**, 024002 (2004); R. A. Konoplya and E. Abdalla, Phys. Rev. D **71**, 084015 (2005); L. Vanzo and S. Zerbini, Phys. Rev. D **70**, 044030 (2004); J. Natario and R. Schiappa, hep-th/0411267.
[9] P. C. Argyres, S. Dimopoulos, and J. March-Russell, Phys. Lett. B **441**, 96 (1998); T. Banks and W. Fischler, hep-th/9906038; S. B. Giddings and S. Thomas, Phys. Rev. D **65**, 056010 (2002); S. Dimopoulos and G. Landsberg, Phys. Rev. Lett. **87**, 161 602 (2001).
[10] P. Kanti and J. March-Russell, Phys. Rev. D **66**, 024023 (2002).
[11] P. Kanti and J. March-Russell, Phys. Rev. D **67**, 104019 (2003).
[12] P. Kanti, Int. J. Mod. Phys. A **19**, 4899 (2004).
[13] D. Ida, K. y. Oda, and S. C. Park, Phys. Rev. D **67**, 064025 (2003); **69**, 049901(E) (2004).
[14] E. Newman and R. Penrose, J. Math. Phys. (N.Y.) **3**, 566 (1962).
[15] S. Chandrasekhar, *The Mathematical Theory of Black Holes* (Oxford University Press, Oxford, 1992).
[16] J. N. Goldberg, A. J. MacFarlane, E. T. Newman, F. Rohrlich, and E. C. Sudarshan, J. Math. Phys. (N.Y.) **8**, 2155 (1967).
[17] S. A. Teukolsky, Phys. Rev. Lett. **29**, 1114 (1972); Astrophys. J. **185**, 635 (1973).
[18] U. Khanal, Phys. Rev. D **28**, 1291 (1983).
[19] B. F. Schutz and C. M. Will, Astrophys. J. Lett. **291**, L33 (1985); S. Iyer and C. M. Will, Phys. Rev. D **35**, 3621 (1987).
[20] R. A. Konoplya, Phys. Rev. D **68**, 024018 (2003); J. Phys. Stud. **8**, 93 (2004).
[21] E. Berti, K. D. Kokkotas, and E. Papantonopoulos, Phys. Rev. D **68**, 064020 (2003).
[22] R. A. Konoplya, Phys. Rev. D **68**, 124017 (2003).
[23] G. L. Gunter, Phil. Trans. R. Soc. A **296**, 497 (1980); **301**, 705 (1981).
[24] K. D. Kokkotas and B. F. Schutz, Phys. Rev. D **37**, 3378 (1988).
[25] V. Ferrari, M. Pauri, and F. Piazza, Phys. Rev. D **63**, 064009 (2001); R. A. Konoplya, Gen. Relativ. Gravit. **34**, 329 (2002); Phys. Rev. D **66**, 084007 (2002).
[26] S. Fernando and C. Holbrook, hep-th/0501138.
[27] R. A. Konoplya, Phys. Rev. D **71** 024038 (2005).
[28] V. Cardoso and J. P. S. Lemos Phys. Rev. D **67**, 084020 (2003).
[29] A. Zhidenko, Classical Quantum Gravity **21**, 273 (2004); R. A. Konoplya and A. Zhidenko, J. High Energy Phys. 06 (2004) 037.
[30] G. T. Horowitz and V. E. Hubeny, Phys. Rev. D **62**, 024027 (2000).
[31] A. Nunez and A. O. Starinets, Phys. Rev. D **67**, 124013 (2003).
[32] R. A. Konoplya, Phys. Rev. D **66**, 044009 (2002).
[33] V. Cardoso, R. Konoplya, and J. P. S. Lemos, Phys. Rev. D **68**, 044024 (2003).
[34] L. E. Simone and C. M. Will, Classical Quantum Gravity **9**, 963 (1992); R. A. Konoplya, Phys. Lett. B **550**, 117 (2002); A. Ohashi and M. Sakagami, Classical Quantum Gravity **21**, 3973 (2004); R. A. Konoplya and A. V. Zhidenko, Phys. Lett. B **609**, 377 (2005).
[35] R. A. Konoplya, Phys. Rev. D **73**, 024009 (2006).